An $\mathrm{N}\log\mathrm{N}$ method for second-order wave loads on a vertical pile

Henrik Bredmose and Antonio Pegalajar-Jurado

DTU Wind Energy, Denmark, hbre@dtu.dk, ampj@dtu.dk

The second-order wave theory offers a welcome improvement to linear wave loads. Due to the quadratic frequency interactions, they are traditionally a magnitude more costly in terms of CPU time. We here present a method for slender vertical circular cylinders that allows their computation at an effort of $O(N \log N)$, similar to linear wave loads.

1 PROBLEM FORMULATION

We consider a vertical circular cylinder of diameter D at a depth h. A Cartesian coordinate system is adopted with the vertical z-axis pointing upwards from the still water level at the cylinder center and the x-axis pointing in the wave direction. The free surface elevation, η, is measured from the still water level in positive z direction. Further, the horizontal and vertical fluid velocities are expressed by a velocity potential such that $(u, w)^T = \nabla\phi$.

Following standard Stokes wave theory analysis, the free surface conditions can be expressed by quantities at $z = 0$ and be combined into

$$\Phi_{tt} + g\Phi_z = -\left(\nabla_H\Phi \cdot \nabla_H\Phi\right)_t - \frac{1}{g^2}\left(\Phi_{tt}^2\right)_t - \frac{1}{g^2}\Phi_{tttt}\Phi_t - \nabla_H^2\Phi\Phi_t. \tag{1}$$

We apply the Rainey (1995) force model plus the standard viscous Morison force

$$F = \int_{-h}^{\eta} \rho\pi R^2 \left[(C_m + 1)\,\dot{u} + C_m w_z u\right] \mathrm{d}z + \int_{-h}^{\eta} \rho R C_D u|u| \mathrm{d}z. \tag{2}$$

This force model contains the contributions from convective accelerations and the axial divergence force. The inertia loads are identical to the recent force model of Kristiansen & Faltinsen (2017) for the wetted part of the cylinder. The two models further contain different point forces at $z = 0$. These, however, are of third-order magnitude and are thus left out here. By a decomposition of the velocity field into its first- and second-order components, we obtain expressions for the first- and second-order force

$$F_1 = \rho\pi R^2 \int_{-h}^{0} (C_m + 1)\, u_{1,t}\, \mathrm{d}z \quad , \quad F_{2D} = \rho R \int_{-h}^{0} C_D u_1 |u_1|\, \mathrm{d}z \tag{3}$$

$$F_{2I} = \rho\pi R^2 \left[\int_{-h}^{0} (C_m + 1)\left(u_{2,t} + u_1 u_{1,x} + w_1 u_{1,z}\right) + C_m w_{1,z} u_1 \mathrm{d}z + (C_m + 1)\eta_1 u_{1,t}|_{z=0}\right] \tag{4}$$

where F_{2I} and F_{2D} are the second-order inertia and drag loads, respectively.

2 THE LINEAR FORCE

We divide the velocity potential into its first- and second-order parts $\phi_{1,2}$ and express ϕ_1 as a double sided Fourier series

$$\phi_1 = \sum_{j=-N}^{N} \hat{B}_j \mathrm{e}^{\mathrm{i}(\omega_j t - k_j x)} \frac{\cosh k_j(z + h)}{\cosh k_j h}. \tag{5}$$

Here N is the number of positive frequencies, t is time and $\omega_j = j\omega_1$ are the angular frequencies. To make the Fourier series real, we further impose $\hat{B}_{-j} = \hat{B}_j^*$ and $k_{-j} = -k_j$. Here * indicates the complex conjugate and k_j are the wave numbers, which satisfy the linear dispersion relation $\omega^2 - gk\tanh kh = 0$. It is now straight forward to obtain the linear force by insertion of (5) into (3) and integration. We may express the result in non-dimensional form by introduction of

$$\Omega = \omega\sqrt{h/g} \quad , \quad \kappa = kh \quad , \quad \tilde{\phi} = \phi\, h^{-3/2} g^{-1/2} \quad , \quad \hat{\tilde{B}} = \hat{B}\, h^{-3/2} g^{-1/2}. \tag{6}$$

We hereby get the below well known result

$$\frac{F_1}{\rho g \pi R^2} = \sum_{j=-N}^{N} (C_a + 1)\mathcal{F}_1 \hat{\tilde{B}}_j \mathrm{e}^{\mathrm{i}(\omega_j t - k_j x)} \qquad \text{with} \qquad \mathcal{F}_1 = \Omega \tanh\kappa, \tag{7}$$

which can be obtained by FFT with an $N \log N$ effort by use of the linear transfer function $\mathcal{F}_1$.

3 THE SECOND-ORDER FORCE

We look first at the force from the second-order acceleration, the first term of F_{2I}. We denote this term F_{21}. To this end, we derive the second-order potential by insertion of (5), into (4). The application of complex, double sided Fourier sums simplifies the calculations considerably, since no distinction between cosine and sinus functions and sub/super harmonics is needed. We thus get

$$\tilde{\phi}_2 = \mathrm{i} \sum_{m=-N}^{N} \sum_{n=-N}^{N} \hat{\tilde{B}}_m \hat{\tilde{B}}_n \mathcal{T}_\Phi \mathrm{e}^{\mathrm{i}((\omega_m+\omega_n)t - (k_m+k_n)x)} \frac{\cosh(k_m+k_n)(z+h)}{\cosh(k_m+k_n)h} \tag{8}$$

with

$$\mathcal{T}_\Phi = \frac{1}{2} \frac{2(\Omega_m + \Omega_n)\left(\Omega_m^2\Omega_n^2 - \kappa_m\kappa_n\right) + \Omega_m\left(\Omega_n^4 - \kappa_n^2\right) + \Omega_n\left(\Omega_m^4 - \kappa_m^2\right)}{\left(\Omega_m + \Omega_n\right)^2 - \left(\kappa_m + \kappa_n\right)\tanh\left(\kappa_m + \kappa_n\right)}. \tag{9}$$

This result is consistent with Sharma & Dean (1981). We next derive F_{21} by vertical integration of $u_{2,t} = \phi_{2,xt}$. Since the vertical structure of $\tilde{\phi}_2$ is expressed explicitly through the $\cosh(k_m+k_n)(z+h)$ term, the integration can be carried out similarly as for F_1. We state the result as

$$\frac{F_{21}}{\rho g \pi R^2 h} = (C_m + 1)\mathrm{i} \sum_{m=-N}^{N} \sum_{n=-N}^{N} \hat{\tilde{B}}_m \hat{\tilde{B}}_n \mathcal{F}_{21} \mathrm{e}^{\mathrm{i}((\omega_m+\omega_n)t - (k_m+k_n)x)} \tag{10}$$

with the quadratic transfer function

$$\mathcal{F}_{21} = \mathcal{T}_\Phi \left(\Omega_m + \Omega_n\right) \tanh\left(\kappa_m + \kappa_n\right). \tag{11}$$

4 NUMERICAL SPEED UP BY EIGENMODE DECOMPOSITION

While (10) is compact, it still requires to evaluate the double summation. We will now show how this can be circumvented by eigenmode decomposition of the quadratic transfer function. We first observe that the double sum for fixed x and t in (10) can be written as a matrix product

$$\frac{F_{21}}{\rho g \pi R^2 h} = (C_m + 1)\mathrm{i} \left[\ldots \hat{\tilde{B}}_m \mathrm{e}^{\mathrm{i}(\omega_m t - k_m x)} \ldots \right] \mathcal{F}_{21} \begin{bmatrix} \vdots \\ \hat{\tilde{B}}_n \mathrm{e}^{\mathrm{i}(\omega_n t - k_n x)} \\ \vdots \end{bmatrix} \tag{12}$$

where $\mathcal{F}_{21}$ here is the $2N \times 2N$ interaction matrix. Next, since $\mathcal{F}_{21}$ is symmetric and quadratic, we can diagonalize it by eigenmode decomposition

$$\frac{F_{21}}{\rho g \pi R^2 h} = (C_m + 1)\mathrm{i} \sum_{j=1}^{2N} \left[\dots \hat{\hat{B}}_m \mathrm{e}^{\mathrm{i}(\omega_m t - k_m x)} \dots \right] \mathbf{V_j} \lambda_j \mathbf{V}_j^T \begin{bmatrix} \vdots \\ \hat{\hat{B}}_n \mathrm{e}^{\mathrm{i}(\omega_n t - k_n x)} \\ \vdots \end{bmatrix} \tag{13}$$

$$= (C_m + 1)\,\mathrm{i} \sum_{q=1}^{2N} \lambda_q \left[\sum_{m=-N}^{N} V_{qm} \hat{\hat{B}}_m \mathrm{e}^{\mathrm{i}(\omega_m t - k_m x)} \right] \left[\sum_{n=-N}^{N} V_{qn} \hat{\hat{B}}_n \mathrm{e}^{\mathrm{i}(\omega_n t - k_n x)} \right] \tag{14}$$

where in the last equation, the product of the $\hat{\hat{B}}\mathrm{e}^{\mathrm{i}(\omega t - kx)}$ vector and eigenvectors of each mode has been recast into the two bracketed sums. We can interpret — and evaluate — these by applying each eigenvector as a transfer function to the potential amplitudes. Hence, with known eigenvectors, this operation can be made at $O(N \log N)$ by FFT, and the two (identical) pseudo timeseries can be multiplied in the time domain. Next, analogous to SVD analysis, we may be able to approximate (14) by truncation of the active modes. Thus for a finite and fixed number of modes, the second-order force can be computed at a computational effort of $O(N \log N)$.

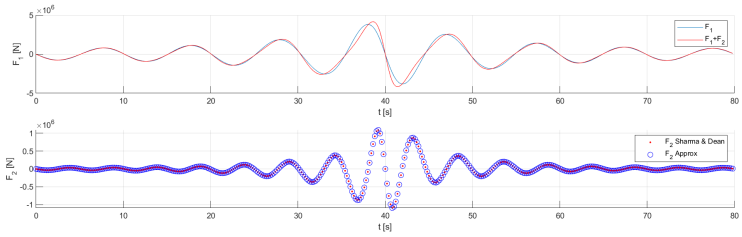

Figure 1: First- and second-order force for a focused wave group. The exact and approximate method (lower).

Figure 1 shows results for a focused wave group and its force at a monopile at 33 depth. We have chosen a JONSWAP spectrum with $T_p = 10$ s, a peak enhancement parameter of $\gamma = 3.3$ and a linear crest height of 6 m. The upper panel show the first- and first+second-order solution calculated with the Sharma & Dean (1981) theory, integrated with 40 points in the vertical. Force coefficients of $(C_m, C_D) = (1.0, 1.0)$ have been used throughout. The lower panel compares the second-order forces of (4) and shows a perfect match at the graphical level. We have calculated the QTF matrix on a 16 x 16 frequencies grid, used 8 modes and interpolated the pseudo transfer functions to the full frequency vector.

5 ACCURACY AND EFFICIENCY

The accuracy of the method relies on an accurate representation of the full QTF matrix. Figure 2 thus shows the QTF matrix for $\mathcal{F}_{2I}$ and the ratio between the approximate and exact matrix for 8 modes. We see that the QTF is quite flat and that the 8 mode approximation is accurate, with noticeable errors only in a low frequency band, where up to 5% error occurs.

We next turn to random realizations of forces from irregular waves. For the same wave condition as in figure 1 time series of 2, 4, ..., 32768 seconds were calculated with the 40 point Sharma & Dean method and the accelerated method, still based on 16-member eigenvectors for 8 modes. A resolution of 0.1 s in time was used. An error measure was defined as $Err = \sigma_{F-F_{\mathrm{SD}}}/\sigma_{F_{\mathrm{SD}}}$. This error is shown in figure 3(a) and shows that the method can compute the inertia loads with an error level of 1.5%, while the drag loads are obtained with an error level of 5%, both independent of the length of the time series. The efficiency of the method is demonstrated in figure 3(b), where the computational time

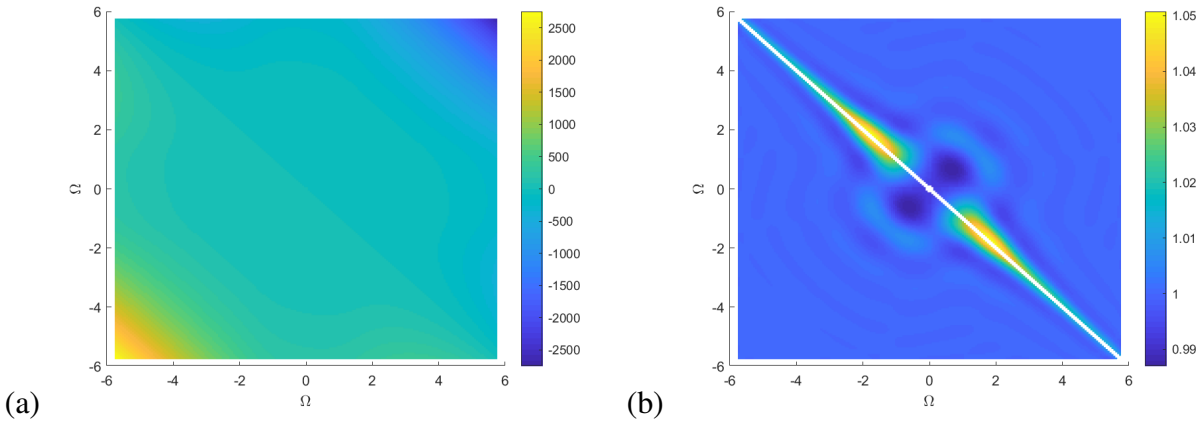

Figure 2: The quadratic transfer function for the full force. (b) The ratio of the approximate and full transfer function.

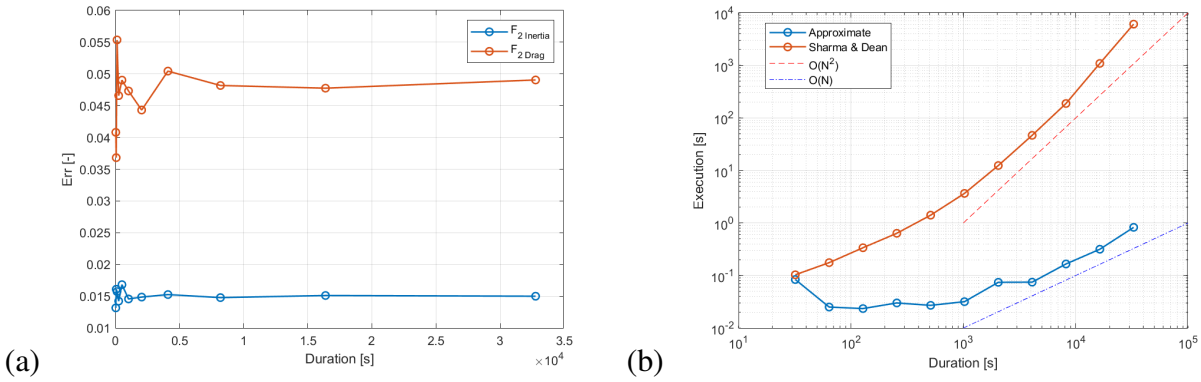

Figure 3: (a) Error as function of time series length. (b) Computational time versus time series length.

in Matlab on a standard laptop is depicted as function of time series length. The calculations also included the moment, which however is omitted here. For the Sharma & Dean method, the Fourier coefficients were summed up at each frequency, such that the actual time series of kinematics can be obtained at an $O(N^2)$ effort. For the approximate method, the CPU usuage scales like N and is always smaller than for the original method. Due to the initial solution of the 16 x 16 eigenvalue problem, the computational time is almost constant at 0.03 s until the interpolation and FFT operations for large time series dominates. The new method is seen to be around 1000 times faster than the conventional method for a 3 hour time series. The speed-up technique of eigendecomposition and interpolation can also be applied to QTFs of panel method output.

The research was supported by the DeRisk project (grant no 4106-00038B) and the FloatStep project (grant no 8055-00075A), both funded by Innovation Fund Denmark. This funding is gratefully acknowledged. Harry Bingham, DTU, is thanked for stimulating input on the dimensionless formulation.

References

Kristiansen, T. & Faltinsen, O. M. (2017), 'Higher harmonic wave loads on a vertical cylinder in finite water depth', *Journal of Fluid Mechanics* **833**, 773–805.

Rainey, R. C. T. (1995), 'Slender-body expressions for the wave load on offshore structures', *Proceedings of the Royal Society of London* **450**(1939), 391–416.

Sharma, J. N. & Dean, R. G. (1981), 'Second-Order Directional Seas and Associated Wave Forces.', *Society of Petroleum Engineers journal* **21**(1), 129–140.